Electromagnetic Modeling of Objects Inside Buildings

Marija M. Nikolić, Antonije R. Djordjević, and Arye Nehorai, *Fellow, IEEE*

***Abstract* — We develop numerical electromagnetic models for computing the response of targets hidden inside buildings. The buildings are electrically large structures whose modeling requires large number of unknowns. We compare two different approaches: exact model based on the method of moments and approximate model that combines the method of moments and ray tracing.**

***Keywords* — Method of moments, ray tracing, through-the-wall sensing.**

I. Introduction

We consider the electromagnetic response of objects located inside buildings and illuminated by exterior sensors. The goal is to develop sophisticated models that capture the individual characteristics of the concealed objects such as shape, material, etc., and yet are amenable to signal processing. Challenges arise from the electrical size of the buildings, whose modeling requires prohibitively large number of unknowns. To reduce the size of the problem, the usual approach combines beamforming with the point-target model [1]. This method is improved in [2] and [3] by taking into account the influence of complex inhomogeneous walls. A more detailed target model based on the physical optics (PO) is proposed in [4]. However, PO is suitable only in the case of electrically large, flat targets. Here, we propose the combination of the ray tracing (RT) and the method of moments (MoM). We substitute the targets and sensors, which require delicate modeling, by their equivalent surface electric and magnetic currents. We take into account the presence of the walls while computing the mutual impedances of the current sources.

Various hybrid models are vastly used in the analyses of scatterers, antennas, and cavities. The algorithm that computes the scattering from perfectly conducting bodies using PO and MoM was derived in [5]. The joint use of FDTD and RT was proposed in [6] for the analyses of fields in cavities. The RT/MoM hybrid aimed for computing the fields scattered from small protrusions on large conducting bodies was developed in [7]. In [8], the authors consider the application of MoM, PO, and RT for the analysis of antennas with large, axially symmetric, dielectric radomes. The scattered field is the sum of the contributions of the currents computed by MoM and PO. However, in the proposed method, the analyses of the radome and the antenna are decoupled. In contrast to that approach, we jointly analyze the sensors and the targets assuming they are in the far-field of the wall. The influence of the wall is considered indirectly when computing the fields from the equivalent surface currents.

We verify the proposed approach by computing the exact response of the building using MoM. The electromagnetic model based on MoM takes into account the multiple reflections among targets and walls, as opposed to the hybrid model.

This work was supported in part by the Serbian Ministry of Science and Technological Development under grant TR 11021, by the COST action IC0603, and by the project F-133 of the Serbian Academy of Sciences and Arts.

M. M. Nikolić and A. R. Djordjević are with the School of Electrical Engineering, University of Belgrade, Belgrade, Serbia (e-mail: mnikolic@etf.rs and edjordja@etf.rs).

Arye Nehorai is with Washington University in St. Louis, St. Louis, MO, USA(e-mail nehorai@wustl.edu).

II. Electromagnetic Modeling

A. MoM Model

In Fig. 1 we show the cross-section of a building with two objects inside. We assume the walls to be made of a homogenous dielectric of relative permittivity ε_r and relative permeability μ_r. The building is surrounded by an array of electromagnetic sensors.

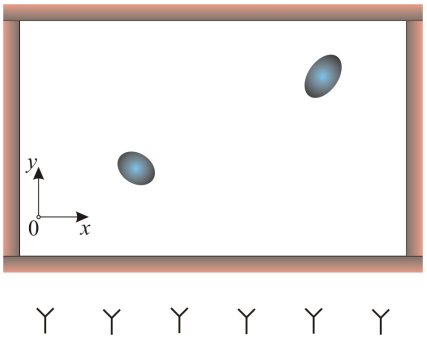

Fig. 1. Hidden objects inside building and sensor array.

We study the two-dimensional (2D) case. The sensors are thin (filamental) conductors, excited by impressed electric fields. We assume that the magnetic field is transverse to the *z*-axis (TM field). As the result of this excitation, the electromagnetic field is established in the whole domain. We solve this inhomogeneous electromagnetic problem by means of the equivalence theorem [9], [10]. By the equivalence theorem, the electromagnetic field outside an arbitrary closed domain remains the same if we replace the domain with equivalent

surface electric and magnetic currents:

$$\mathbf{J}_S = \mathbf{n} \times \mathbf{H}, \quad (1)$$

$$\mathbf{M}_S = -\mathbf{n} \times \mathbf{E}, \quad (2)$$

where $\mathbf{J}_s$ is the vector of the equivalent surface electric currents, $\mathbf{M}_s$ is the vector of the equivalent surface magnetic currents, $\mathbf{H}$ is the magnetic field vector at the domain boundary (interface), $\mathbf{E}$ is the electric field vector at the interface, and $\mathbf{n}$ is the unit normal vector pointing outside the domain. (In the TM case, the electric currents are axial, and the magnetic currents are circumferential.) The equivalent currents, together with exterior sources, produce zero field inside the body. Hence, we can fill that region by an arbitrary medium without affecting the EM field outside the considered domain [9], [10].

In the problem at hand, we apply the equivalence theorem on each of following domains (entities): building walls, targets, and sensors. Firstly, we substitute all the entities with their equivalent surface currents. If we assume that a vacuum is inside each entity (zero-field region), we have an electromagnetic problem with a homogeneous medium (vacuum). The excitation of the sensors is modeled by an impressed electric field ($\boldsymbol{E}_i$). We show the sketch of the equivalent (exterior) problem in Fig. 2.

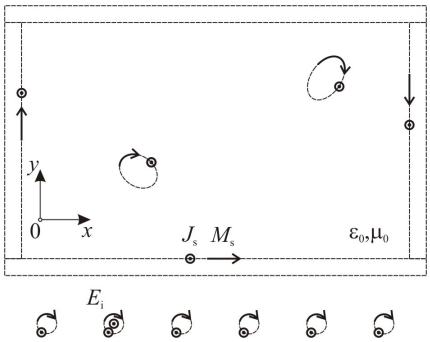

Fig. 2. Application of equivalence theorem – exterior problem.

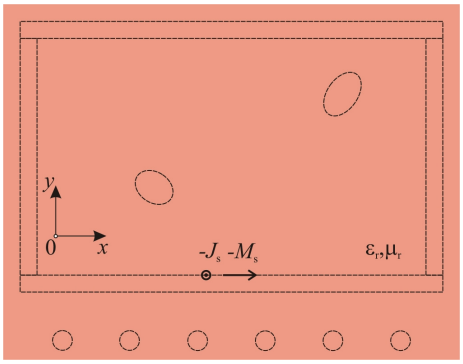

Fig. 3. Application of equivalence theorem – interior problem.

In the second case, we consider each entity separately. We refer to those problems as the interior problems. The equivalent currents with the same magnitude as in the previous case (J_s , M_s), but opposite in direction, produce the exact field inside the considered entity and zero field outside the entity [9], [10]. Hence, we substitute the region outside the entity with the same dielectric as the one inside the entity. We illustrate this in Fig. 3 for the building wall next to the sensors. The sources of the electromagnetic field in this case are the surface electric and magnetic currents on the interface of the considered entity. (The other entities have no influence.) The currents are placed in a homogeneous dielectric, as shown in Fig. 3.

We compute the unknown currents using the electric-field integral equation (EFIE) [9], [11]. The electric field expressed in terms of the potentials reads

$$\mathbf{E} = -\mathrm{j}\omega\mathbf{A} - \frac{1}{\varepsilon}\mathrm{curl}\,\mathbf{F} + \mathbf{E}_\mathrm{i}, \quad (3)$$

where $\mathbf{A}$ is the magnetic vector-potential, $\mathbf{F}$ is the electric vector-potential, $\mathbf{E}_\mathrm{i}$ is the impressed electric field, and ε is the permittivity of the medium. (The grad V term is missing because the electric currents are z-directed, with no z-variation. Hence, there are no electric charges associated with the currents.) The potentials are given by

$$\mathbf{A} = \mu \int_s \mathbf{J}_\mathrm{S}\, g(r)\, \mathrm{d}s, \quad (4)$$

$$\mathbf{F} = \varepsilon \int_s \mathbf{M}_\mathrm{S}\, g(r)\, \mathrm{d}s, \quad (5)$$

where g is Green's function, r is the distance between the field point and the observation point, and s is the circumference of the boundary surfaces where the currents are located. In the exterior problem, the medium is a vacuum and Green's function is

$$g(r) = -\frac{\mathrm{j}}{4} H_0^{(2)}(kr), \quad (6)$$

where $H_0^{(2)}$ is the Hankel function of the second kind and order zero and $k = \omega\sqrt{\varepsilon_0\mu_0}$ is the phase coefficient in a vacuum. In the interior problems, Green's functions are

$$g_i(r) = -\frac{\mathrm{j}}{4} H_0^{(2)}(-\mathrm{j}\gamma_i r), \quad (7)$$

where $\gamma_i = \mathrm{j}\omega\sqrt{\varepsilon_i\mu_i}$ is the propagation coefficient in the considered entity. For good conductors, (7) can also be written in the form $g_i(r) = \frac{1}{2\pi}\left[\ker(|\gamma_i|r) + \mathrm{j}\,\mathrm{kei}(|\gamma_i|r)\right]$, where ker and kei are the Kelvin functions, $\gamma_i = \sqrt{\mathrm{j}\omega\sigma_i\mu_i}$, and σ_i is the conductivity.

We use the pulse expansion to approximate the unknown current distribution. To that purpose, we divide all boundary surfaces (i.e., the surfaces of sensors, dielectric, and targets) into a number of line segments and assume that the currents are uniformly distributed along each segment:

$$J(x,y) \approx \sum_{i=1}^{N} J_i f_i(x,y), \quad (8)$$

$$M(x,y) \approx \sum_{i=1}^{N} M_i f_i(x,y), \quad (9)$$

with

$$f_i(x,y)=\begin{cases}1 \text{ on the } i\text{th segment}\\ 0 \text{ otherwise}\end{cases}, \tag{10}$$

where J_i is the electric-current coefficient on the ith segment, M_i is the magnetic-current coefficient on the ith segment, and N is the total number of segments. We show the implementation of the pulse expansion for the currents in Fig. 4.

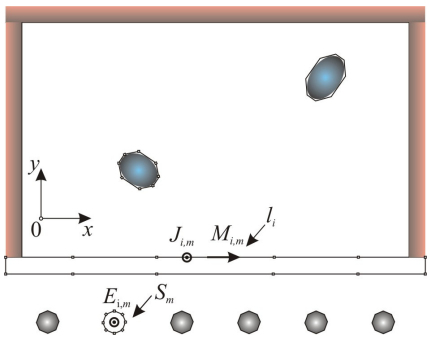

Fig. 4. Pulse expansion for currents.

The electric field due to the electric-current source on the ith segment reads

$$E(\mathbf{r})=-\mathrm{j}\omega\mu J_i\int_{s_i} g(r)\,\mathrm{d}s \tag{11}$$

and the field due to the magnetic-current source is

$$E(\mathbf{r})=M_i\int_{s_i}\frac{\mathrm{d}g}{\mathrm{d}r}\mathbf{u}_i\times\mathbf{u}_r\,\mathrm{d}s\,, \tag{12}$$

where s_i is the ith segment, $\mathbf{r}$ is the position-vector of the observation point, $\boldsymbol{u}_r$ is the unit vector in the radial direction, and $\boldsymbol{u}_i$ is the unit vector in the direction of the segment s_i.

We use the point-matching technique to compute the unknown current coefficients [9], [11]. For the exterior problem, we impose the condition that the electric field is zero on the inner side of the surfaces of all entities. In the interior problems, we impose the condition that the electric field is zero on the outer side of the entity's surface. The total number of the linear equations is $2N$. The matching points are located at the segment midpoints. The resulting system of equations when the mth sensor is excited reads

$$\mathbf{e}_m=G\mathbf{j}_m\,, \tag{13}$$

$$\mathbf{j}_m=\begin{bmatrix}\mathbf{j}_{\mathrm{s}\,m}^T & \mathbf{m}_{\mathrm{s}\,m}^T\end{bmatrix}^T, \tag{14}$$

where $G\in C^{2N\times 2N}$ is the system matrix, $\mathbf{j}_{\mathrm{s}m}\in C^{N\times 1}$ is the vector of the unknown electric currents, $\mathbf{m}_{\mathrm{s}m}\in C^{N\times 1}$ is the vector of the unknown magnetic currents, $\mathbf{e}_m\in C^{2N\times 1}$ is the excitation vector. The (k,l) entry of the matrix G represents the electric field produced by a constant unit electric or magnetic $\mathbf{j}_i[l]$ at the matching point $\boldsymbol{r}_k$. The excitation vector contains the values of the impressed field at the matching points. The excitation of the sensors is important only in the exterior problem. We assume that only sensors can be excited, i.e.,

$$\mathbf{e}_m[k]=\begin{cases}1 \text{ if } \mathbf{r}_m \text{ is on the } m\text{th sensor}\\ 0 \text{ otherwise}\end{cases}. \tag{15}$$

B. Hybrid Model

We now consider the computation of the electromagnetic response of the targets inside the building using the hybrid approach. We apply MoM procedure described in the previous subsection on the equivalent system without the walls, shown in Fig. 5.

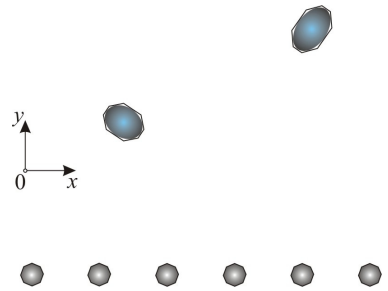

Fig. 5. Equivalent system used in the hybrid model.

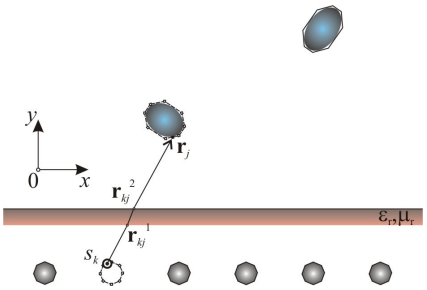

Fig. 6. Computation of electric field.

We substitute the targets and sensors by their equivalent surface electric and magnetic currents. We formulate the system of equations for the unknown equivalent currents using the pulse expansion and point matching. In contrast to MoM modeling, we do not substitute the walls with their equivalent surface currents. Instead, we consider the influence of the walls when computing the electric field produced by current sources on the segments. We illustrate this approach in Fig. 6, in which we show the case with only one wall. We consider two current sources on the opposite sides of the wall. The electric field at the matching point $\mathbf{r}_j$ on the target due to the current of segment S_k on the sensor is approximately given by

$$E^h(\mathbf{r}_j)=E(\mathbf{r}_j)\frac{D_0}{D_{\mathrm{wall}}}T_{12}T_{21}\exp\left(-\mathrm{j}2\pi f(\tau_{\mathrm{wall}}-\tau_0)\right), \tag{16}$$

$$\tau_{\mathrm{wall}}=\left(\left|\mathbf{r}_j-\mathbf{r}_{jk}^1\right|+\left|\mathbf{r}_{jk}^2-\mathbf{r}_{jk}^1\right|\sqrt{\varepsilon_{\mathrm{r}}}+\left|\mathbf{r}_k-\mathbf{r}_{jk}^2\right|\right)/c_0\,, \tag{17}$$

$$\tau_0=\left|\mathbf{r}_j-\mathbf{r}_{jk}^1\right|/c_0\,, \tag{18}$$

$$D_0=\sqrt{\left|\mathbf{r}_j-\mathbf{r}_k\right|}\,, \tag{19}$$

where $E(\mathbf{r}_j)$ is the electric field in the case without the wall, $\mathbf{r}_{jk}^1$ and $\mathbf{r}_{jk}^2$ are the refraction points, T_{12} is the transmission coefficient of the air-dielectric boundary, T_{21} is transmission coefficient of the dielectric-air boundary, D_0 is the spatial attenuation (spreading factor) of the ray

connecting the segment S_k and the matching point $\mathbf{r}_j$ in vacuum, D_{wall} is the spreading factor in the presence of the wall, τ_0 is the time delay in vacuum, and τ_{wall} is the time delay with the wall in a scene. The number of the unknown coefficients is the same as for the target in a vacuum. However, the computational complexity is increased because of the numerical calculation of the refraction points and the spreading factor.

III. Example

We consider a metallic target with square cross-section and side length a (Fig. 7). The target is hidden behind a homogeneous dielectric wall of permittivity $\varepsilon_r = 3$. The wall length is 8 m and the thickness is 0.2 m. The center of the target has Cartesian coordinates $(0.2\,\text{m}, 1\,\text{m})$. We assume that the target is illuminated by a thin electric conductor placed at $(0\,\text{m}, 1\,\text{m})$. We compute the surface currents on the target circumference for $a = 30$ cm and $a = 40$ cm. We show the results in Fig. 8.

We obtained very good agreement for $a = 30$ cm, although the target is in the vicinity of the wall (the far-field zone of the target is $4a^2/\lambda = 1.2$ m). As expected, the discrepancy increases as the target becomes larger and closer to the wall.

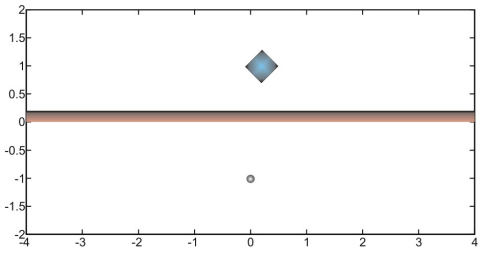

Fig. 7. Experimental setup.

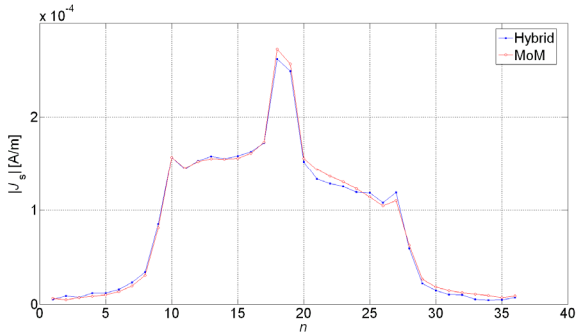

Fig. 8. Surface electric-current density along target circumference ($a = 0.3$ m).

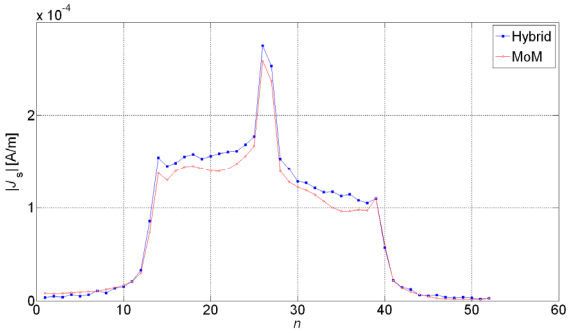

Fig. 9. Surface electric-current density along target circumference ($a = 0.4$ m).

IV. Conclusion

We computed the response of objects hidden behind walls using MoM and using an approximate method that combines MoM and ray tracing. We showed that the approximate method can be efficiently employed if the target is sufficiently separated from the wall.

References

[1] F. Ahmad, M.G. Amin, and S.A. Kassam, "Synthetic aperture beamformer for imaging through a dielectric wall," *IEEE Trans. Aerosp. Electron. Syst.*, Vol. 41, No. 1, Jan. 2005, pp. 271–283.

[2] M.M. Nikolić, A. Nehorai, and A.R. Djordjević, "Estimating Moving Targets Behind Reinforced Walls Using Radar," *IEEE Trans. Antennas Propagat.*, Vol. 57, No. 11, Nov. 2009, pp. 3530-3538.

[3] M. Dehmollaian, "Hybrid electromagnetic models for the purpose of detection and identification of visually obscured targets," *PhD thesis*, The University of Michigan, 2007.

[4] T. Dogaru and C. Le, *Validation of Xpatch Computer Models for Human Body Radar Signature*, Army Research Laboratory, 2008.

[5] U. Jakobus and F.M. Landstorfer, "Improved PO-MM hybrid formulation for scattering from three-dimensional perfectly conducting bodies of arbitrary shape," *IEEE Trans. Antennas Propagat*, Vol. 43, No. 2, Feb. 1995, pp.162-169.

[6] R. Lee and T. Chia, "Analysis of electromagnetic scattering from a cavity with a complex termination by means of a hybrid ray-FDTD method," *IEEE Trans. Antennas Propagat.*, Vol. 41, No. 11, pp. 1560-1569, Nov 1993.

[7] J.M Jin, L. Feng, S.T. Carolan, J.M. Song, W.C. Gibson, W.C. Chew, L. Cai-Cheng, and R. Kipp, "A hybrid SBR/MoM technique for analysis of scattering from small protrusions on a large conducting body," *IEEE Trans. Antennas Propagat.,* Vol. 46, No. 9, Sep 1998, pp. 1349-1357.

[8] M.A.A. Moneum, Z. Shen, J.L. Volakis, and O. Graham, "Hybrid PO-MoM analysis of large axi-symmetric radomes," *IEEE Trans. Antennas Propagat.*, vol. 49, no. 12, Dec. 2001, pp. 1657-1666.

[9] A.R. Djordjević, T.K. Sarkar, and S.M. Rao "Analysis of finite conductivity cylindrical conductors excited by axially-independent TM electromagnetic field," *IEEE Microwave Theory Techn.*, Vol. 33, No. 10, Oct. 1985, pp. 960–966.

[10] R.F. Harrington, *Time-Harmonic Electromagnetic Fields*, McGraw-Hill, New York, 1961.

[11] R.F. Harrington, *Field Computation by Moment Methods*, Krieger Publishing Co., Malabar, FL, 1982.